AN APPROACH BASED ON GAMMA-RAY TRANSMISSION TECHNIQUE AND ARTIFICIAL NEURAL NETWORK FOR ACCURATELY MEASURING THE THICKNESS OF VARIOUS MATERIALS

by

Le Thi Ngoc TRANG [1,2,3]***, Nguyen Thi Truc LINH*** [1,2,3]***,***
Tran Thien THANH [2,3]***, Hoang Duc TAM*** [4]***, and Huynh Dinh CHUONG*** [1,2,3*]

[1] Nuclear Technique Laboratory, University of Science, Ho Chi Minh City, Vietnam
[2] Faculty of Physics and Engineering Physics, University of Science, Ho Chi Minh City, Vietnam
[3] Vietnam National University, Ho Chi Minh City, Vietnam
[4] Faculty of Physics, Ho Chi Minh City University of Education, Ho Chi Minh City, Vietnam

Scientific paper
https://doi.org/10.2298/NTRP2402098T

This paper presents an approach based on the gamma-ray transmission technique and artificial neural network for accurately measuring the thickness of various materials in flat sheet form. The gamma-ray transmission system comprises a NaI(Tl) scintillation detector coupled with a ^{137}Cs radioactive source. The artificial neural network model predicts the sample thickness through three input features: mass density, linear attenuation coefficient, and ln(R) – where R represents the ratio of areas under the 662 keV peak in spectra acquired from measurements with and without the sample. The artificial neural network model was trained using simulation data generated by MCNP6 code, facilitating the creation of comprehensive datasets covering diverse material types and thickness variations at a low cost. Hyperparameters of the artificial neural network model were defined by several optimization methods, such as hyperband-bayesian, tree-structured Parzen estimator, and random search, to establish an optimal artificial neural network architecture. Subsequently, the optimal artificial neural network model was deployed to predict the thickness of graphite, aluminum, copper, steel, and polymethyl methacrylate sheets, using input data obtained from the experiments. The results showed a good agreement between predicted and reference thicknesses, with a maximum relative deviation of 1.94 % and an average relative deviation of 0.52 %.

Key words: artificial neural network, flat sheet, gamma-ray transmission, thickness measurement

INTRODUCTION

Flat sheets of various materials are extensively applied across numerous modern industries, serving as fundamental components for a multitude of products and structures. In automotive manufacturing, they form crucial parts like body panels and chassis components. In shipbuilding, they form vital structures such as ship hulls, decks, and bulkheads. Within aerospace, they contribute to the construction of aircraft fuselages and wings. Furthermore, in construction and furniture, they are used for crafting items like tabletops, shelves, cabinet doors, and others.

Previous studies [1-3] have shown the thickness effect on the mechanical properties of different materials. These findings emphasize the importance of adhering to prescribed thickness standards to mitigate safety risks and ensure optimal performance when using flat sheets. Therefore, it is essential to detect and eliminate unsatisfactory input materials before they enter the production line or assess the quality of flat-rolled products at the output of the production line. Accurate monitoring and characterization of the thickness help to enhance product quality and increase manufacturing efficiency. This task requires non-destructive techniques that operate consistently and continuously even under harsh conditions of industrial environments to accurately measure the thickness of diverse materials.

Nowadays, various non-destructive techniques have been developed to measure the thickness of flat sheets, spanning from a few millimeters to several centimeters. These techniques rely on different physical principles, including ultrasonic [4], eddy current [5, 6], and gamma rays [7-13]. Each technique has its

* Corresponding author, e-mail: hdchuong@hcmus.edu.vn

own set of advantages and disadvantages. When choosing a thickness measurement technique for a specific application, factors such as precision, cost, thickness range, and sample composition should be considered. Among the aforementioned techniques, the gamma- -ray transmission (GT) technique [7-10] stands out for its unique advantages that are particularly suitable for monitoring the thickness of flat sheets in industrial production processes. The GT technique relies on the attenuation of gamma-ray beam intensity as it passes through an absorbing sample to determine the thickness. Therefore, this technique applies to all material types and is less susceptible to variations in environmental factors and surface conditions of the sample. Meanwhile, the ultrasonic technique is less effective for highly attenuative or porous materials, and the eddy current technique cannot be applied to non-conductive materials. Both ultrasonic and eddy current techniques may be affected significantly by environmental factors such as temperature, humidity, and electromagnetic interference [14, 15]. Moreover, the ultrasonic technique is sensitive to the surface conditions of the sample, roughness on the surface can affect the accuracy of ultrasonic thickness measurements [16]. In industrial settings, materials under examination are diverse, such as metals, plastics, composites, rocks, woods, glasses, and more. Environmental factors frequently fluctuate as well. Both ultrasonic and eddy current techniques are not as suitable as the GT technique for such dynamic industrial environments. Regarding the use of gamma-rays in non-destructive testing, the gamma-ray back-scattering (GBS) technique has also been successfully deployed to measure the thickness of flat sheets [11-13]. In comparison to the GBS measurements, the GT measurements typically yield much higher counting rates under identical conditions of radioactive source and detector. Therefore, the GT technique is better suited than the GBS technique for continuously monitoring thickness in real time. In summary, from our perspective, the GT technique is most effective and suitable for monitoring the thickness of flat sheets in industrial production processes.

Over the years, researchers have continuously developed various analytical methods to enhance the precision and versatility of thickness gauges using the GT technique. Shirakawa [7] proposed a nonlinear model for determining the thickness of steel sheets. This model was based on using the effective linear attenuation coefficient (LAC) to address the buildup factor in GT measurements. Measurements were performed on steel reference samples ranging from 0.35 cm to 10 cm in thickness, using a system equipped with a ^{137}Cs radioactive source and a gas detector. Using the experimental data, the author applied an exponential function to fit the relationship between the effective LAC and the thickness of steel sheets. This enabled the thickness determination of steel sheets based on gamma-ray counts recorded by the detector. Chuong *et al*. [8] used MCNP6 code to simulate a GT system, featuring a ^{137}Cs radioactive source and a NaI(Tl) scintillation detector. The simulation spectra showed a strong agreement with experimental spectra across various thicknesses and material types of flat sheets. Subsequently, the simulation data were utilized to establish linear calibration curves by fitting the values of ln$R$ with the sample thickness. Here, R represents the ratio of areas under the 662 keV peak in spectra acquired from measurements with and without the sample. The thickness of flat sheets under examination was determined based on these linear calibration curves. It should be emphasized that each specific type of material requires its calibration curve for accurate thickness determination. Variations in the composition or density of the sample can invalidate previously established calibration curves. Therefore, the analytical methods described in references [7, 9] face limitations in cases where a calibration curve for the material under examination is unavailable. To address this challenge, Chuong *et al.* [10] expanded the simulations to cover a diverse range of materials. Based on the simulation results, the authors demonstrated a correlation between the slope coefficient of the linear calibration curves and the LAC of the samples. From there, a mathematical equation was established to determine the sample thickness based on ln$R$ and LAC values. Santos *et al.* [9] presented a methodology based on the GT technique and artificial neural network (ANN) to measure the thickness of some metal alloys. Using simulation data generated by the MCNP6 code, the authors established several ANN models and evaluated their performance in predicting thickness. The results indicated that an ANN model using input data consisting of the area under the 662 keV peak and density of the sample produced accurate predictions of thickness. Specifically, in 91.2 % of all cases examined, the relative errors were below 1 %. For the remaining cases, the relative errors ranged from 1 % to 5 %, all of which were associated with thin samples. This demonstrates the feasibility of integrating the GT technique with ANN for predicting the thickness of different materials. However, the focus of this study [9] is confined to some metal alloys like aluminum, titanium, and carbon steel alloys. To expand the analysis to encompass a wider range of materials, relying only on the area under the 662 keV peak and the sample density as input data for the ANN model is insufficient for accurate thickness prediction. Indeed, interactions between gamma rays with an energy of 662 keV and matter involve two main mechanisms: the Compton scattering (cross-section is proportional to Z) and the photoelectric absorption (cross-section is proportional to Z^5). The presence of elements with high atomic numbers in the material composition can significantly affect the attenuation of a 662 keV gamma-ray beam. Therefore, it is necessary to account for the influence of material composition in the ANN model.

The ANN is a mathematical model that can learn complex patterns and relationships from finite training datasets. Given an adequate training dataset, the ANN

can generalize correlations between output outcomes and input variables, even when these correlations are not apparent or exhibit clear trends. This ability enables accurate predictions of interested information across various complex scenarios. In recent years, ANN has emerged as a powerful tool for multivariate quantitative analysis that involves the consideration of multiple variables and their interactions with one another. Evaluating the capabilities and effectiveness of ANN in various fields of nuclear science and technology is highly meaningful. A previous study [17] has confirmed that the ANN-based analytical method brings notable improvements compared to earlier methods for the efficiency calibration of HPGe detectors. Therefore, it is expected that the integration of the ANN model with the GT technique will significantly enhance the precision of thickness measurements for flat sheets made from diverse materials. This motivation drove us to conduct the present study.

The main goal of the present study is to develop an ANN model for accurately predicting the thickness of various materials, using input data obtained from GT measurements with a ^{137}Cs radioactive source and a NaI(Tl) scintillation detector. To perform this study, we first used Monte Carlo simulations with the MCNP6 code to generate the pulse height distribution (PHD) spectra for GT measurements across various thicknesses and materials of the sample. Through analysis of the spectra, we determined the ln(R) values, and an ANN model was constructed to predict the sample thickness. The dataset obtained from simulations was used for training and validating the ANN model. Finally, experimental measurements were conducted on several materials, including graphite, aluminum, copper, steel, and polymethyl methacrylate (PMMA), to provide data for testing the ANN model. The precision of the ANN model is evaluated through the deviations between the predicted and reference thicknesses. Additionally, the precision of the ANN model has been compared to that of the calibration curve fitting (CCF) method described in reference [10].

MATERIALS AND METHODS

Experiments

To measure the thickness of flat sheets, we established a GT system comprising a source block and a detector block, as shown in fig. 1. The source block includes a ^{137}Cs radioactive source with an activity of 18.5 MBq contained within a cylindrical lead collimator with a diameter of 1 cm and a length of 10 cm. This block produces a narrow beam of 662 keV gamma-rays that precisely targets the center of the detector block. The detector block consists of a NaI(Tl) scintillation detector housed within a cylindrical lead collimator with a diameter of 1 cm and a length of 2 cm. The distance between the source block and the detector block is 37 cm.

The NaI(Tl) scintillation detector used in this study has crystal dimensions of 7.62 cm × 7.62 cm and an energy resolution of 7.3 % at the 662 keV peak. The detector was connected to an Osprey unit and a computer to form a gamma-ray spectrometer. The Osprey is a versatile tube base for scintillation detectors, incorporating the high-voltage power supply, amplifier, and digital multichannel analyzer. The multichannel analyzer was operated in 2048-channel mode. Recorded signals are transmitted from the Osprey to the computer via a USB cable, with spectral acquisitions controlled by GENIE-2000 software version 3.3.

We conducted thickness measurements on flat sheets made from five commonly used industrial materials, including graphite, aluminum, copper, steel, and polymethyl methacrylate (PMMA). These sheets have dimensions of 10 cm × 30 cm, with thicknesses varying as: 0.5 cm to 10 cm for graphite, 0.194 cm to 12.09 cm for aluminum, 0.2 cm to 8.966 cm for copper, 0.59 cm to 9.416 cm for steel, and 1.0 cm to 12.0 cm for PMMA. The thicknesses of all the sheets were measured using a digital caliper with an uncertainty of 0.001 cm. The results obtained from these measurements were used as reference thicknesses to verify the reliability of the ANN model. Additionally, the mass density and LAC of these

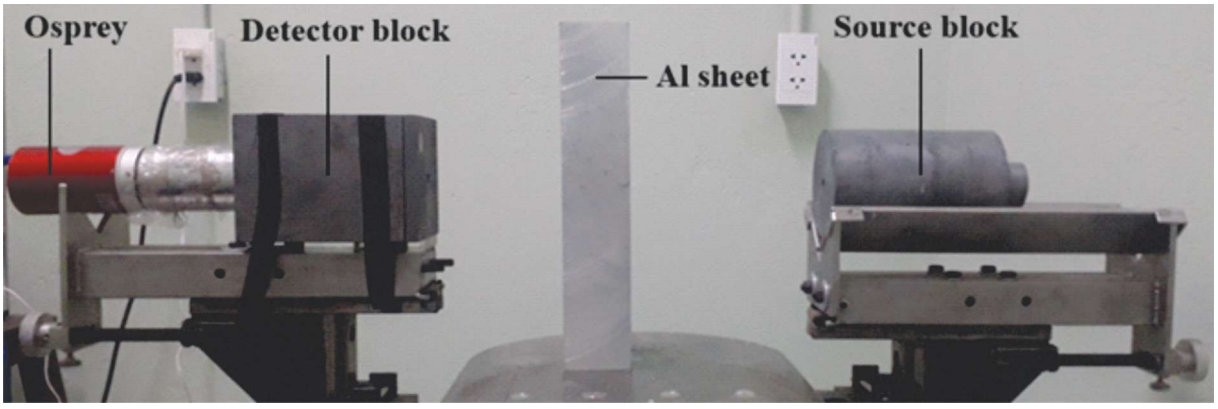

Figure 1. Experimental setup of the GT system for measuring the thickness of flat sheets

Table 1. The mass density and LAC of the flat sheets used in the experiments

Material	Mass density [gcm^{-3}]	LAC [cm^{-1}]
Graphite	1.81	0.1398
Aluminum	2.70	0.2016
Copper	8.96	0.6506
Steel	7.85	0.5827
PMMA	1.16	0.0967

materials were measured on several standard samples, as presented in tab. 1. The mass density was calculated as the ratio of mass to volume. The LAC was determined using the Lambert-Beer law in gamma-ray attenuation measurements.

For the GT measurements, the sheet was positioned on a table so that its surface was perpendicular to the symmetry axes of both the source block and the detector block. The distance from the source block to the front surface of the sheet was consistently maintained at 18.4 cm. Each sheet was measured three times, with an acquisition time of 4000 seconds per measurement. In total, 246 measurements were conducted in this study. Besides, measurements were also performed without a sheet present.

Monte Carlo simulations

To train an ANN model, a comprehensive training dataset is essential. Therefore, we needed to collect a large amount of data from GT measurements for flat sheets with different thicknesses and compositions. However, collecting experimental data is often constrained by the difficulties involved in preparing standard samples with precise thicknesses and compositions. It is not feasible to create a training dataset entirely from experiments. In situations where experimental measurements are inconvenient or impractical, the Monte Carlo simulation method is an excellent solution for generating the necessary data to train an ANN model. Over the years, several general-purpose Monte Carlo codes, such as MCNP [18], GEANT [19], and PENELOPE [20], *etc*., have been developed to simulate the transport of radiations in 3-D geometries. These codes accurately model the interactions of radiation with all materials across a wide range of energies. By utilizing one of these codes, simulations of GT measurements can be conducted easily and cost-effectively.

In this study, the MCNP6 code was used to generate the PHD spectra for the NaI(Tl) scintillation detector in GT measurements. To do this, we created a simulation model (input file) based on the existing GT system, as illustrated in fig. 2. In this simulation model, the geometrical parameters are meticulously and precisely described to match those of the actual GT system. The radioactive source was modeled to emit photons with an energy of 661.657 keV. It is important to note that the specifications of the NaI(Tl) scintillation detector were thoroughly benchmarked in our previous study [21].

The simulation model takes into account the interaction processes of photons with matter, including the photoelectric effect, Compton scattering, Rayleigh scattering, pair production, and fluorescence. The photon interaction and atomic relaxation databases are sourced from ENDF/B-VI.8. The cut-off energy for photon transport is set at 1 keV. Besides, the characteristics of the PHD spectrum recorded by the NaI(Tl) scintillation detector were also carefully considered. The *tally F8* and *FT8 GEB a b c* cards were used simultaneously to produce simulated spectra that closely match the experimental spectra. The energy bins in the simulated spectra were configured to correspond to the channels in the experimental spectra. The *a*, *b*, and *c* parameters accurately characterize the full width at half maximum (FWHM) of peaks across various energies of incident photons.

To ensure a diverse dataset for training the ANN model, we conducted simulations for GT measurements on 34 different types of materials. These included 21 single-element materials and 13 multi-element materials, with effective atomic numbers ranging from 6 to 83. Most of these materials are commonly used in industry. The mass density and LAC of these materials are presented in tab. 2, with LAC values calculated using the XCOM program [22]. For each material, the thickness of flat sheets varied from 0.2 cm to 12 cm. In cases involving materials with high mass density and atomic number, the intensity of the transmitted gamma-ray beam was almost completely attenuated, causing the simulation to stop when the thickness of the flat sheet was less than 12 cm. In each simulation, the histories of 10 billion source particles were tracked to obtain the PHD spectrum with high statistical accuracy. In total, we performed 772 simulations corresponding to various materials and thicknesses of the flat sheets.

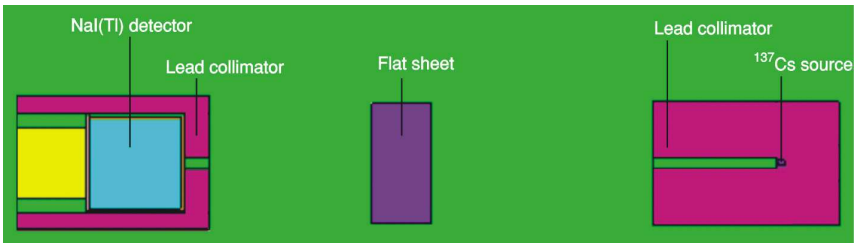

Figure 2. Simulation model of the GT system using MCNP6 code

Table 2. The mass density and LAC of the flat sheets used in the Monte Carlo simulations

Material	Mass density [gcm^{-3}]	LAC [cm^{-1}]	Material	Mass density [gcm^{-3}]	LAC [cm^{-1}]
Graphite	1.70	0.1312	Platinum	21.45	2.2265
Aluminum	2.70	0.2016	Gold	19.32	2.0479
Titanium	4.54	0.3266	Lead	11.35	1.2508
Iron	7.87	0.5786	Bismuth	9.75	1.0975
Copper	8.96	0.6506	Rubber	0.92	0.0793
Zinc	7.14	0.5229	Polyethylene (PE)	0.93	0.0819
Germanium	5.32	0.3770	Polytetrafluoroethylene (PTFE)	2.25	0.1669
Zirconium	6.51	0.4762	Pyrex glass (PG)	2.23	0.1716
Silver	10.50	0.8013	Granite rock (GR)	2.69	0.2063
Tin	7.31	0.5526	2090-T83 Aluminum	2.59	0.1928
Terbium	8.23	0.7156	7075-T6 Aluminum	2.81	0.2096
Thulium	9.32	0.8568	3003-O Aluminum	2.73	0.2038
Lutetium	9.84	0.9263	Concrete	2.30	0.1814
Hafnium	13.31	1.2647	C95800 Copper	7.64	0.5578
Tantalum	16.65	1.6071	C27000 Copper	8.47	0.6171
Tungsten	19.3	1.8879	321 Stainless Steel	8.0	0.5884
Iridium	22.42	2.2936	S45C Steel	7.85	0.5770

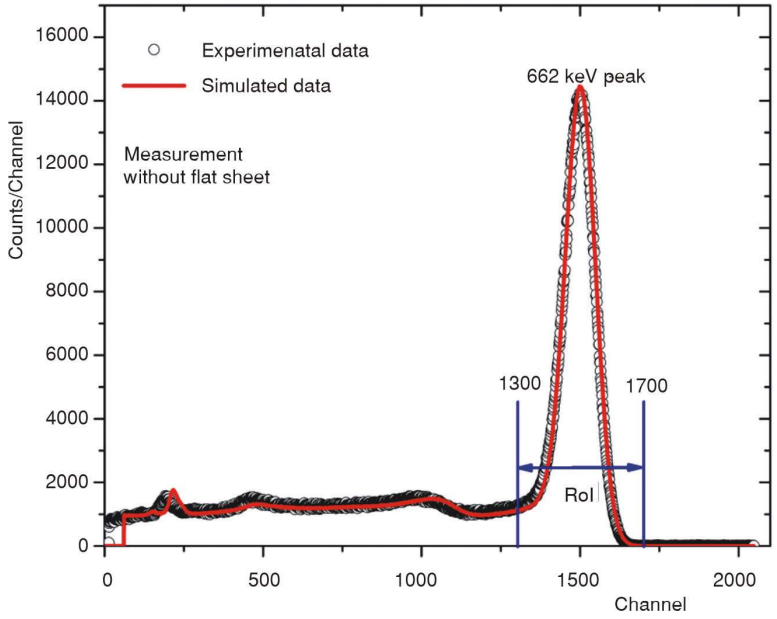

Figure 3. The RoI in the experimental and simulated spectra

Data analysis

A two-step data analysis process was conducted to collect the necessary data for training, validation, and testing of the ANN model. In the first step, we analyzed the PHD spectra obtained from both experiments and simulations to determine the areas under the 662 keV peak. Initially, a region of interest (RoI) was selected, spanning from channel 1300 to channel 1700 in each spectrum, as illustrated in fig. 3. Note that the width from the peak center (approximately channel 1500) to the RoI boundaries is roughly four times the standard deviation of the peak. This means that 99.9936 % of the events, where the 662 keV gamma-rays deposited all of their energy in the detector, were recorded within the RoI. Then, the area under the 662 keV peak was calculated by summing the counts within the RoI.

In the second step, the R^{Exp} and R^{Sim} ratios were calculated as follows

$$R^{Exp} = \frac{N^{Exp}}{N_0^{Exp}} \quad (1)$$

$$R^{Sim} = \frac{N^{Sim}}{N_0^{Sim}} \quad (2)$$

where N^{Exp} and N_0^{Exp} are the areas under the 662 keV peak in the experimental spectra for GT measurements taken with and without flat sheet, respectively, N^{Sim} and N_0^{Sim} and are the areas under the 662 keV peak in the simulated spectra for GT measurements taken with and without flat sheet, respectively. Then, we determined the values of $\ln(R^{Exp})$ and $\ln(R^{Sim})$. These values serve as one of the input variables in the ANN model.

It is necessary to emphasize the significance of using the R ratio in this study. Some differences between experiment and simulation are inevitable. These differences arise from several factors: the uncertainty of the radioactive source activity, the precision of the Monte Carlo code in modeling interactions of radiation with matter, and the accuracy of nuclear databases (such as gamma-ray emission intensity and radioactive half-life). This can result in unignorable deviations between N^{Exp} and N^{Sim}. Therefore, we did not use N^{Sim} as input data for the ANN model. Instead, we found that the R ratio can be employed to eliminate the influence of the aforementioned factors, thereby providing an excellent agreement between experimental and simulated results. Indeed, many previous studies [8, 10, 23-26] demonstrated that the R^{Sim} ratio is reliable enough to replace the R^{Exp} ratio for constructing calibration curves or training ANN models.

ARTIFICIAL NEURAL NETWORKS

Multi-layer perceptron model

In this study, we developed a multi-layer perceptron (MLP) model to accurately predict the thickness of various flat sheets, as illustrated in fig. 4. The MLP is a fundamental type of ANN that simulates the biological neural network in the human brain. Its architecture comprises an input layer, one or more hidden layers, and an output layer. Each of these layers contains nodes, also referred to as neurons, which serve as the basic units for processing data within the network. The input layer comprises three neurons, each neuron representing a specific input feature: ln(R), mass density, and LAC. The hidden layers are positioned between the input and output layers. Each hidden layer performs complex computations and transformations on the inputs received from the previous layer. The number of hidden layers and the number of neurons per hidden layer can vary depending on the specific application and complexity of the problem. The output layer comprises a single neuron that produces the final prediction for the thickness of the flat sheet.

The operation of the MLP model begins with assigning initial weights and biases to the connections between neurons. These weights and biases are initialized randomly. The learning process occurs through the forward and backward propagation of data between the interconnected neurons. In the forward propagation phase, the input data is processed at the input layer and passed to the first hidden layer. Each neuron in the hidden layer receives inputs from the previous layer, computes a weighted sum of these inputs, adds a bias term, and then applies an activation function. The activation function introduces non-linearity into the network, enabling it to learn complex relationships and patterns. The result of each neuron is then passed to the neurons in the next layer, continuing until the data reaches the output layer. Finally, the neuron in the output layer produces the thickness predictions. The difference between these predictions and the actual target values across the entire dataset, known as the loss, is quantified using the mean squared error (MSE) as a loss function. Subsequently, the backward propagation phase is conducted to adjust the weights and biases within the network, aiming to minimize the loss. This process propagates the error gradient backward through the network, starting from the output layer and moving towards the input layer. The gradient of the loss function is calculated concerning each weight and bias, thereby indicating the direction and magnitude of the necessary adjustments to reduce the loss. Using the adaptive moment estimation (ADAM) optimization al-

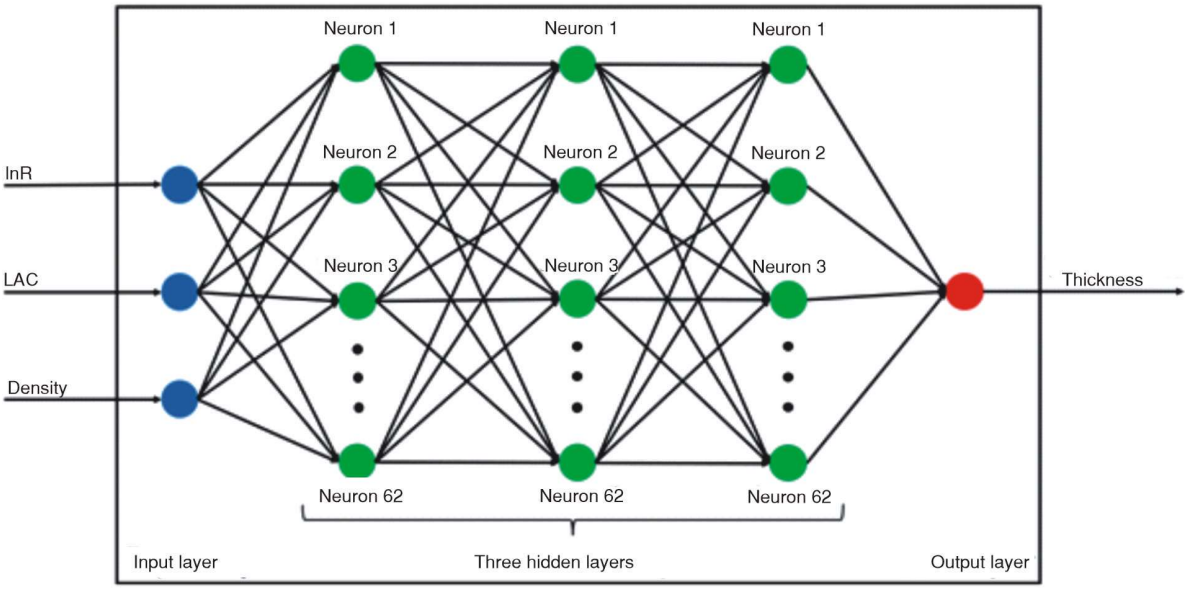

Figure 4. The MLP architecture developed in this study for predicting the thickness of flat sheets

gorithm, weights and biases are then updated in the direction that decreases the loss. Lower loss values indicate better model performance, enabling the model to make more accurate predictions and effectively capture the underlying relationships in the data. Forward and backward propagation are repeated over many iterations, known as epochs, to improve the performance of the MLP model.

Evaluating the performance of an MLP model is essential to ensure its accuracy and reliability in making predictions. This task requires the use of various statistical metrics, including MSE, mean absolute percentage error (MAPE), and coefficient of determination (R^2). These metrics are defined as follows

$$MSE = \frac{1}{n} \cdot \sum_{i=1}^{n} (d_i^{\text{ref}} - d_i^{\text{pred}})^2 \tag{3}$$

$$MAPE = \frac{100}{n} \cdot \sum_{i=1}^{n} \left| \frac{d_i^{\text{ref}} - d_i^{\text{pred}}}{d_i^{\text{ref}}} \right| \tag{4}$$

$$R^2 = 1 - \frac{\sum_{i=1}^{n} (d_i^{\text{ref}} - d_i^{\text{pred}})^2}{\sum_{i=1}^{n} (d_i^{\text{ref}} - \overline{d^{\text{pred}}})^2} \tag{5}$$

where d_i^{ref} and d_i^{pred} are the i^{th} reference thickness and the i^{th} predicted thickness, respectively; $\overline{d^{\text{pred}}}$ – the average of all predicted values, and n – the number of data points.

Training, validation, and testing datasets

All data obtained from the experiments and simulations were divided into three subsets: training, validation, and testing datasets. Each subset serves a distinct purpose in the MLP model development process.

The training dataset is used to train the MLP model. This dataset consists of simulated data, which provides the primary data foundation for the model to understand and generalize the relationships within the problem to be solved. Figures 5(a) and 5(b) display the values of $\ln(R^{\text{Sim}})$ corresponding to various materials and thicknesses included in the training dataset. Information about the mass density and LAC of the materials used in the training dataset can be found in tab. 2. The training dataset comprises 611 data points, accounting for 79 % of all data generated from the simulations.

The validation dataset is used to tune the hyperparameters of the MLP model and to prevent overfitting. This dataset is composed of simulation data that is entirely separate from the training dataset. Figure 6 displays the values of $\ln(R^{\text{Sim}})$ corresponding to various materials and thicknesses included in the validation dataset. Information about the mass density and LAC of the materials used in the validation dataset can be found in tab. 2. The validation dataset comprises 161 data points, accounting for 21 % of all data generated from the simulations. These data points are not used directly in the training process but serve as checkpoints to periodically evaluate the performance of the MLP model. This helps ensure that the model generalizes well to new and unseen data.

The testing dataset is used after the ANN model has been fully trained to evaluate its final performance. To provide an unbiased assessment of the predictive power of the trained MLP model and generalization capabilities in real-world scenarios, the testing dataset is composed entirely of experimental data. Figure 7 shows the values of $\ln(R^{\text{Exp}})$ corresponding to various materials and thicknesses included in the testing dataset, which consists of 246 data points. Information about the mass density and LAC of the materials used in the testing dataset can be found in tab. 1.

Hyperparameter optimization

In the MLP models, crucial hyperparameters include the number of hidden layers, the number of neurons per hidden layer, the activation functions, the learning rate, the batch size, and the number of epochs. These hyperparameters are predefined and remain constant throughout the training process. They influence the learning process and performance of the MLP model. Therefore, selecting the optimal hyperparameters is a critical step in developing an effective MLP model. However, finding the optimal values for hyperparameters is a complex process because the values of some hyperparameters can depend on others. This interdependence creates numerous optimization opportunities, requiring researchers to spend significant time surveying and evaluating different combinations.

Fortunately, several optimization techniques have been developed to automatically identify the optimal values for hyperparameters. In this study, we applied three optimization techniques, including hyperband-bayesian, tree-structured Parzen estimator, and random search, to determine various sets of optimal hyperparameter values. This approach helps save time and computational resources while enhancing the performance of the MLP model. The hyperparameter search space was established as:

- The activation function is chosen from the following options: tanh, softsign, sigmoid, linear, and selu.
- The number of hidden layers varies from 1 to 5.
- The number of neurons within each hidden layer varies from 3 to 100.
- The batch size varies from 6 to 100.
- The learning rate varies from 10^{-6} to 10^{-2}.
- The number of epochs remains constant at 1000.

For each optimization technique, the process of finding optimal hyperparameters was run 100 times, and the best result among these runs was selected. Therefore, we have obtained three different sets of optimal hyperparameter values, as presented in tab. 3.

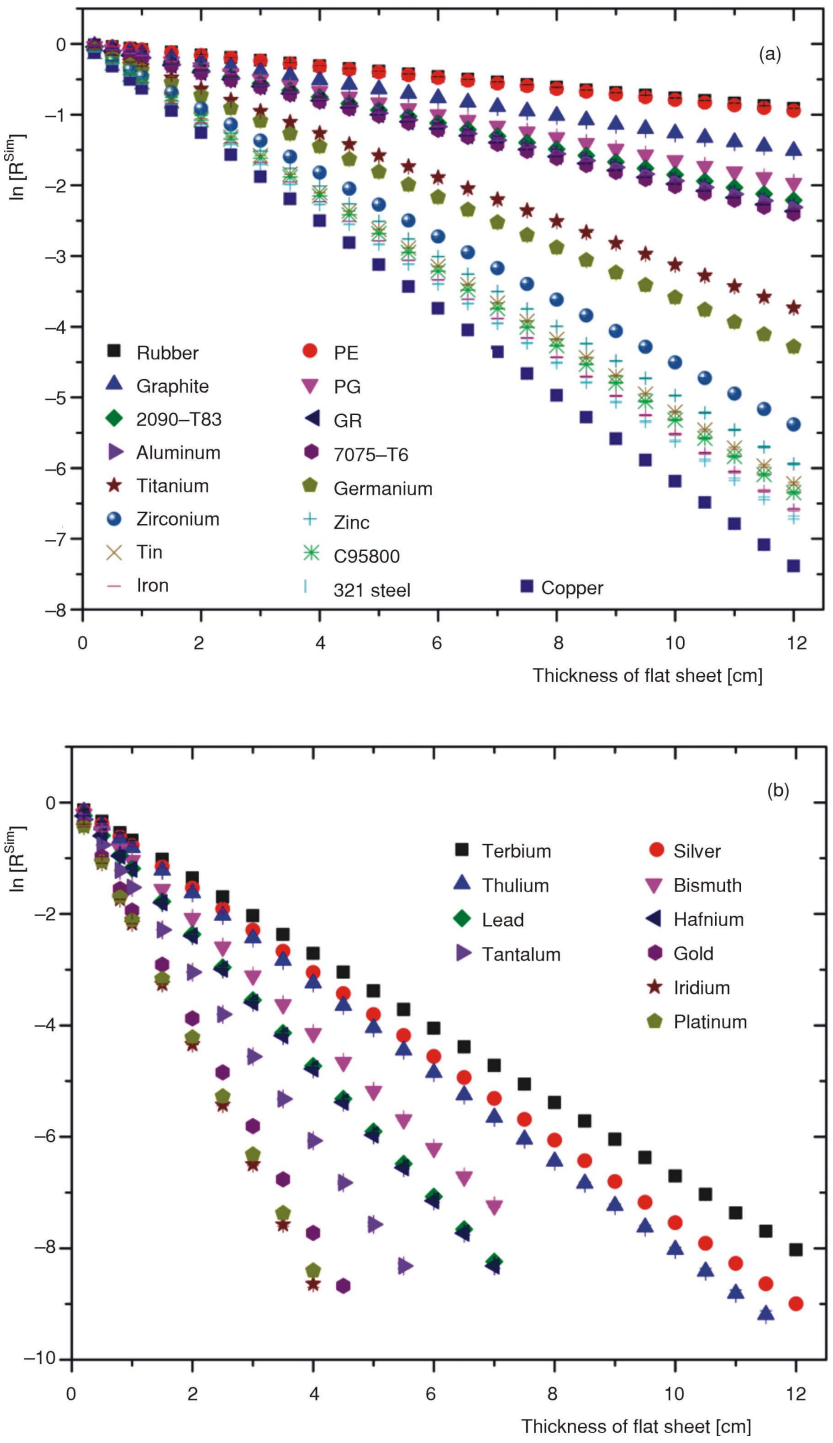

Figure 5. Data points of ln(R^{Sim}) in the training dataset

Subsequently, MLP models were trained based on these sets of optimal hyperparameter values. From the trained MLP models, we computed statistical metrics, such as MSE, MAPE, and R^2, on both the training and validation datasets. The criteria for selecting the optimal MLP model are the lowest MSE and MAPE, along with an R^2 value closest to 1. As shown in tab. 3, the MLP model optimized with the tree-structured Parzen estimator technique exhibited the best statistical metrics. These metrics confirm that the model achieves high accuracy and reliability in predicting the thickness of flat sheets. Furthermore, the training process shows no indications of overfitting. Consequently, this model was selected for predicting the thickness of flat sheets in real-world scenarios.

RESULTS AND DISCUSSIONS

We applied the trained MLP model to predict the thickness of various flat sheets based on input data collected from experiments (testing data). Figure 8 dis-

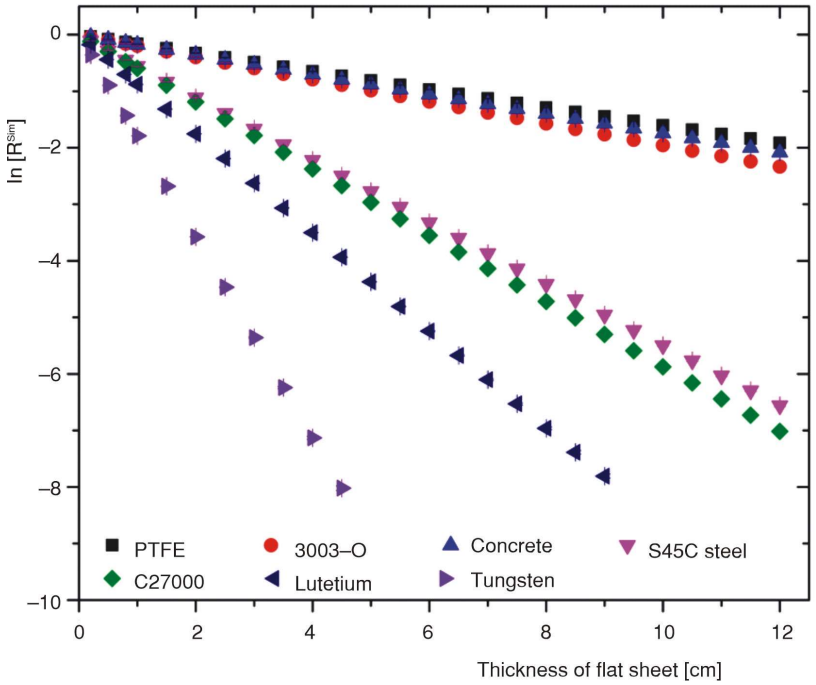

Figure 6. Data points of ln(R^{Sim}) in the validation dataset

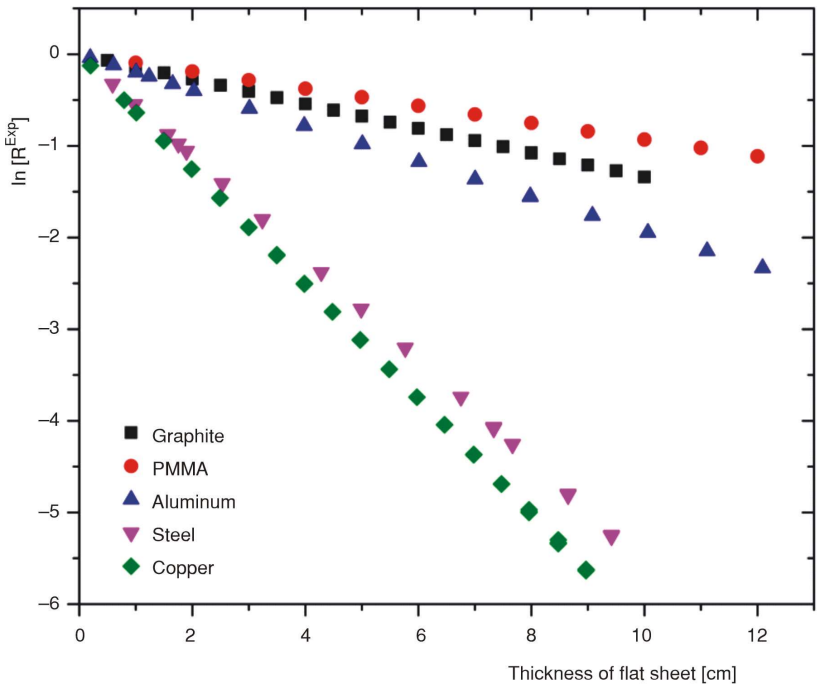

Figure 7. Data points of ln(R^{Exp}) in the testing dataset

plays the comparison between the reference and predicted thicknesses, clearly showing that the predicted values align closely with the reference values. The statistical metrics reveal an MSE of 0.1299, a MAPE of 0.5173, and an R^2 of 0.9999. Additionally, all relative deviations (RD) between the predicted and reference thicknesses are less than 2.0 %. These results confirm the precision of the trained MLP model for predicting the thickness of flat sheets in practical settings.

Besides, the CCF method, as described in reference [10], has been applied to determine the thickness of flat sheets. To do this, the simulation data were utilized to construct a calibration curve, and experimental data were employed to evaluate the precision of the method. Figure 9 shows the RD between the reference thicknesses and the thicknesses determined by the ANN and CCF methods across five different materials. In general, the RD with the ANN method are smaller than those with the CCF method in most cases.

Table 3. The sets of optimal hyperparameter values determined by the optimization techniques and their statistical metrics

Description of parameters	Values obtained based on various optimization techniques		
	Hyperband-Bayesian	Tree-structured Parzen Estimator	Random Search
Activation function	Tanh	Softsign	Tanh
Number of hidden layers	3	3	3
Number of neurons per hidden layer	61	62	122
Batch size	12	36	67
Learning rate	0.0003129	0.0011666	0.0096071
MSE for the training dataset	0.1463	0.0854	0.2690
MAPE for the training dataset	0.880	0.7439	1.2494
R^2 for the training dataset	0.9999	0.9999	0.9998
MSE for validation dataset	0.1210	0.0619	0.1668
MAPE for validation dataset	0.8287	0.6468	1.1204
R^2 for validation dataset	0.9999	1.0	0.9999

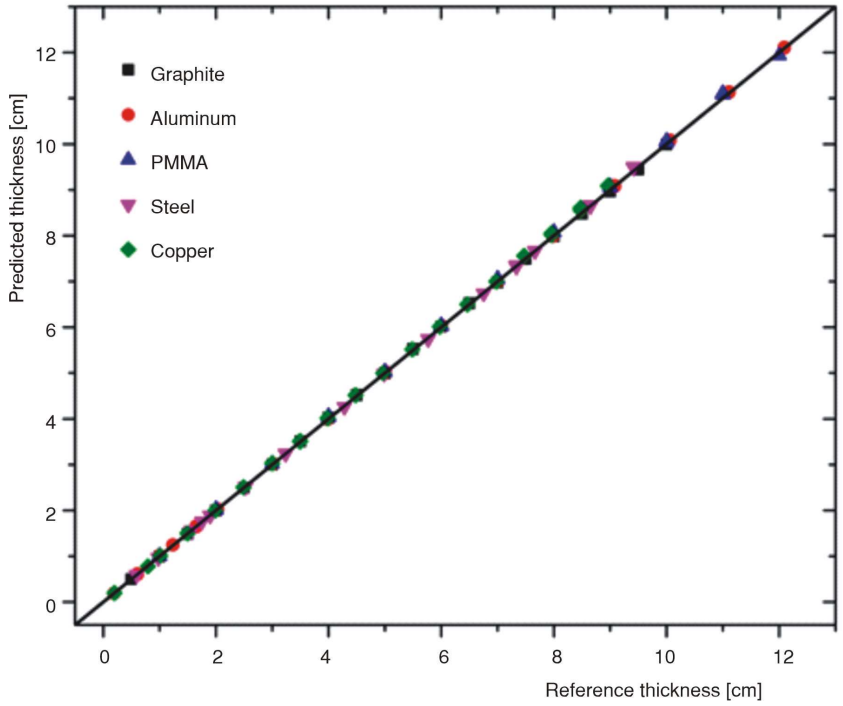

Figure 8. Comparison between reference thicknesses and predicted thicknesses using the MLP model across five distinct materials in the testing dataset

Furthermore, both the average RD and maximum RD with the ANN method are significantly lower than those with the CCF method, as presented in tab. 4. An exception is observed for the PMMA material, for which we currently lack a definitive explanation. However, this exception does not substantially affect the overall trend observed. Based on these results, it is evident that the ANN method provides more accurate outcomes compared to the CCF method for the GT system used.

It should be noted that the thickness measurements obtained through the CCF method in this study did not achieve the same level of accuracy as those reported in reference [10]. This discrepancy can be attributed to differences in the measuring geometries. In the current set-up, the collimators have a larger diameter and a shorter length compared to the previous configuration. Such changes in geometry could compromise the linear relationship essential for calibration curves. Consequently, for measurement geometries involving *poor collimators*, using the ANN method is recommended to enhance the precision for thickness measurements. The term *poor collimators* refers to collimators characterized by a large diameter and a short length.

CONCLUSIONS

In the present study, we propose an approach that combines the GT technique (using a ^{137}Cs radioactive source and a NaI(Tl) scintillation detector) with ANN to measure the thickness of flat sheets made from diverse materials. The results confirm the feasibility of our approach for providing accurate predictions of thickness. Indeed, the very low relative deviations between the reference and predicted thicknesses, with an average of 0.52 % and a maximum of 1.94 % across in-

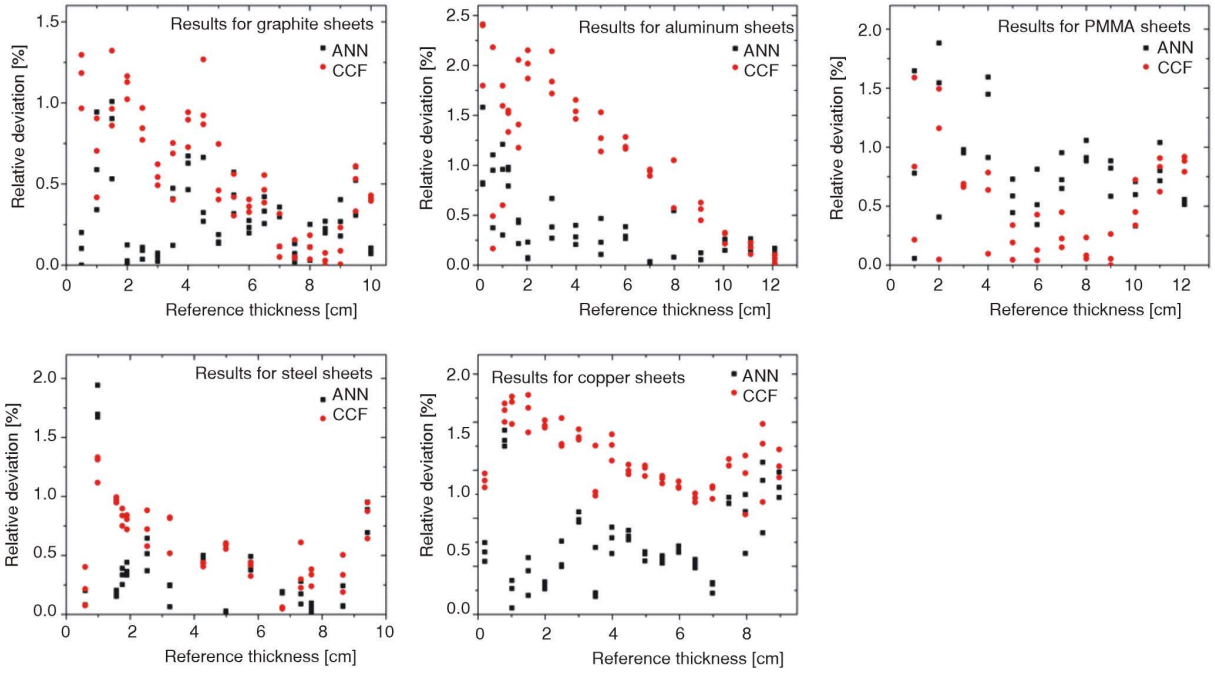

Figure 9. The relative deviations between reference thicknesses and thicknesses determined by the ANN and CCF methods across five different materials

Table 4. The average and maximum relative deviations obtained from the ANN and CCF methods

Material	ANN method		CCF method	
	Average RD [%]	Maximum RD [%]	Average RD [%]	Maximum RD [%]
Graphite	0.29	1.01	0.55	1.32
Aluminum	0.40	1.58	1.15	2.41
PMMA	0.83	1.88	0.50	1.59
Steel	0.39	1.94	0.59	1.33
Copper	0.76	1.92	1.63	2.28
All materials	0.52	1.94	0.92	2.41

vestigated materials, demonstrate the excellent reliability of this approach. Furthermore, the strengths of our approach lie in the simplicity of the data analysis process and the robust ability of the MLP model to generalize the relationships between input variables and desired outputs. Using the Monte Carlo simulation method, the necessary data for training the MLP model can be flexibly and cost-effectively generated. These advantages underscore the significant potential of this approach for practical implementation.

Besides, this study shows that using ANN significantly enhances accuracy compared to the previously developed CCF method. We predict that these improvements will be even more pronounced in cases where the GT system is not equipped with good collimators. In such cases, the linear relationships in the calibration curves may not be maintained, leading to decreased accuracy in the CCF method. Therefore, it is recommended to use the ANN method for measurement geometries that involve *poor collimators*.

ACKNOWLEDGMENT

This research is funded by Vietnam National University, Ho Chi Minh City (VNU-HCM) under grant number C2022-18-09.

AUTHORS' CONTRIBUTIONS

L. T. N. Trang: literature review, ANN model developing, data analysis, manuscript correction, project administration. H. D. Chuong: research idea proposing, experiments, simulations, original manuscript writing. N. T. T. Linh: experiments, data analysis, manuscript correction. T. T. Thanh: material providing, manuscript correction. H. D. Tam: simulations, manuscript correction.

ORCID NO

Le Thi Ngoc Trang: 0000-0002-9354-022X
Huynh Dinh Chuong: 0000-0003-3903-6388
Nguyen Thi Truc Linh: 0000-0002-7706-8391
Tran Thien Thanh: 0000-0002-9866-4926
Hoang Duc Tam: 0000-0001-8880-8810

REFERENCES

[1] Suh, C. H., *et al*., Effects of Thickness and Surface Roughness on Mechanical Properties of Aluminum Sheets, *J. Mech. Sci. Technol., 24* (2010), Nov., pp. 2091-2098

[2] Qiu, T., *et al*., Thickness Effect on the Mechanical Properties of Nacre in Hyriopsis Cumingii Under Three-Point Bending, *Eng. Fract. Mech., 276* (2022), Dec., 108869
[3] Qiu, T., *et al*., Research on the Thickness Effect and Micro-Fracture Mechanism of Graphite Sheets with Layered Structures, *Diam. Relat. Mater., 143* (2024), Mar., 110908
[4] Waag, G., *et al*., Air-Coupled Ultrasonic Through-Transmission Thickness Measurements of Steel Plates, *Ultrasonics, 56* (2015), Feb., pp. 332-339
[5] Cheng, W., Thickness Measurement of Metal Plates Using Swept-Frequency Eddy Current Testing and Impedance Normalization, *IEEE Sens. J., 17* (2017), 14, pp. 4558-4569
[6] Lu, M., *et al*., Thickness Measurement of Non-Magnetic Steel Plates Using a Novel Planar Triple-Coil Sensor, *NDT E Int., 107* (2019), Oct., 102148
[7] Shirakawa, Y., A Build-Up Treatment for Thickness Gauging of Steel Plates Based on Gamma-Ray Transmission, *Appl. Radiat. Isot., 53* (2000), 4-5, pp. 581-586
[8] Chuong, H. D., *et al*., Thickness Determination of Material Plates by Gamma-Ray Transmission Technique Using Calibration Curves Constructed from Monte Carlo Simulation, *Radiat. Phys. Chem., 190* (2022), Jan., 109821
[9] Santos, A. G. M., *et al*., Thickness Prediction in Metal Alloys Using Nuclear Techniques and Artificial Neural Network: Modelling, *Appl. Radiat. Isot., 191* (2023), Jan., 110531
[10] Chuong, H. D., *et al*., A Novel Approach for Constructing the Calibration Curve Applied in Determining the Thickness of Different Types of Materials, *Radiat. Phys. Chem., 214* (2024), Jan., 111282
[11] Tam, H. D., *et al*., Advanced Gamma Spectrum Processing Technique Applied to the Analysis of Scattering Spectra for Determining Material Thickness, *J. Radioanal. Nucl. Chem., 303* (2015), Jan., pp. 693-699
[12] Nguyen, V. H., *et al*., New Method for Processing Gamma Backscattering Spectra to Estimate Saturation Depth and to Determine Thickness of Aluminum and Steel Materials, *J. Radioanal. Nucl. Chem., 315* (2018), Feb., pp. 293-298
[13] Chuong, H.D., *et al*., A New Approach for Determining the Thickness of Material Plate Using Gamma Backscattering Method, *NDT E Int., 113* (2020), July, 102281
[14] Panda, K. G., *et al*., Effects of Environment on Accuracy of Ultrasonic Sensor Operates in Millimetre Range, *Perspect. Sci., 8* (2016), Sept., pp. 574-576
[15] Bato, M. R., *et al*., Impact of Human and Environmental Factors on the Probability of Detection During NDT Control by Eddy Currents, *Measure., 133* (2019), Feb., pp. 222-232
[16] Benstock, D., *et al*., The Influence of Surface Roughness on Ultrasonic Thickness Measurements, *J. Acoust. Soc. Am., 136* (2014), 6, pp. 3028-3039
[17] Chuong, H. D., *et al*., A Comparative Study on Full-Energy Peak Efficiency Calibration Methods for HPGe Detector: Virtual Point Detector, Curve Fitting, and Machine Learning Models, *Nucl. Instrum. Methods Phys. Res. A, 1058* (2024), Jan., 168941
[18] Goorley, T., *et al*., Features of MCNP6, *Ann. Nucl. Energy, 87* (2016), 2, pp. 772-783
[19] Agostinelli, S., *et al*., Geant4 - A Simulation Toolkit, *Nucl. Instrum. Methods Phys. Res. A, 506* (2003), 3, pp. 250-303
[20] Baró, J., *et al*., PENELOPE: An Algorithm for Monte Carlo Simulation of the Penetration and Energy Loss of Electrons and Positrons in Matter, *Nucl. Instrum. Methods Phys. Res. B, 100* (1995), 1, pp. 31-46
[21] Sang, T. T., *et al*., Simple Procedure for Optimizing Model of NaI(Tl) Detector Using Monte Carlo Simulation, *J. Radioanal. Nucl. Chem., 322* (2019), Nov., pp. 1039-1048
[22] Berger, M. J., *et al*., NIST XCOM: Photon Cross Sections Database, https://www.nist.gov/pml/xcom-photon-cross-sections-database
[23] Chuong, H. D., *et al.*, Monte Carlo Simulation Combined with Experimental Measurements Based on Gamma Transmission Technique for Determining the Density of Liquid, *Radiat. Phys. Chem., 179* (2021), Feb., 109216
[24] Linh, N. T. T., *et al*., Combining Monte Carlo Simulation and Experimental Data for Determining the Density of Polymer Materials in Gamma Scattering and Gamma Transmission Measurements, *J. Radioanal. Nucl. Chem., 332* (2023), May, pp. 2929-2943
[25] Sang, T. T., *et al*., ANN Coupled with Monte Carlo Simulation for Predicting the Concentration of Acids, *Appl. Radiat. Isot., 169* (2021), Mar., 109563
[26] Tam, H. D., *et al*., Estimation of Liquid Density Using Artificial Neural Network in Gamma-Ray Scattering Measurement, *Nucl Technol Radiat., 37* (2022), 1, pp. 31-41

Received on June 10, 2024
Accepted on September 24, 2024

**Ле Ти Нгок ТРАНГ, Нгујен Ти Трук ЛИЊ, Тран Тин ТАЊ,
Хоанг Дук ТАМ, Хујњ Дињ ЦУЕНГ**

ПОСТУПАК ЗАСНОВАН НА ТЕХНИЦИ ПРЕНОСА ГАМА ЗРАЧЕЊА И ВЕШТАЧКОЈ НЕУРОНСКОЈ МРЕЖИ ЗА ПРЕЦИЗНО МЕРЕЊЕ ДЕБЉИНЕ РАЗЛИЧИТИХ МАТЕРИЈАЛА

Приказан је приступ заснован на техници преноса гама зрачења и вештачкој неуронској мрежи за прецизно мерење дебљине различитих материјала у облику равног листа. Систем за пренос гама зрачења садржи NaI(Tl) сцинтилациони детектор повезан са ^{137}Cs радиоактивним извором. Модел вештачке неуронске мреже предвиђа дебљину узорка преко три улазне карактеристике: густине масе, линеарног коефицијента слабљења и ln(R) – где R представља однос површина испод пика од 662 keV у спектрима добијеним мерењима са и без узорка. Модел вештачке неуронске мреже увежбан је коришћењем симулационих података генерисаних MCNP6 кодом, олакшавајући креирање свеобухватних скупова података који покривају различите врсте материјала и варијација дебљине по ниској цени. Хиперпараметри модела вештачке неуронске мреже дефинисани су помоћу неколико метода оптимизације, као што су хипербанд-Бајесова, дрво-структурирани Парзенов естиматор и случајна претрага, да би се успоставила оптимална архитектура вештачке неуронске мреже. Потом је примењен оптимални модел вештачке неуронске мреже да би се предвидела дебљина листова графита, алуминијума, бакра, челика и полиметил метакрилата, користећи улазне податке добијене из експеримената. Резултати су показали добро слагање између предвиђених и референтних дебљина, са максималним релативним одступањем од 1,94 % и просечним релативним одступањем од 0,52 %.

Кључне речи: вештачка неуронска мрежа, равна плоча, пренос гама зрачења, мерење дебљине